DTC Improvement for Induction Motor Ripples Reduction by Increasing the Number of Sectors

Yassine Zahraoui[1]*, Mohamed Moutchou[1], Souad Tayane[1], Chaymae Fahassa[2], and Sara Elbadaoui[2]

[1]LCCPS Laboratory, Higher National School of Arts and Crafts (ENSAM), Hassan II University, Casablanca 20670, Morocco
[2]Electrical Engineering Department, Mohammadia School of Engineering (EMI), Mohammed V University, Rabat 765, Morocco
*Corresponding author: yassine.zahraoui1-etu@etu.univh2c.ma

OPEN ACCESS

Abstract: This paper presents a modified version of the direct torque control (DTC) in order to improve the performance of the induction motor (IM) operation. The main goal is to reduce the high ripples that constitute the major drawbacks, and which lead to an acoustical noise and degrade the performance of the control scheme, especially at low-speed regions. The augmentation of the number of sectors is a very useful solution, the modified DTC provides a constant switching voltage frequency. This technique reduces the high ripples level in the torque and the flux in spite of its complexity. The twelve sectors DTC with a modified switching table is an effective solution. The obtained results are satisfactory and the performance of the proposed strategy is improved. The results of all the discussed aspects have been obtained by numerical simulation using MATLAB/Simulink.

Keywords: Induction Motor; New Switching Table; Performance Improvement; Ripples Reduction; Twelve Sectors DTC; Total Harmonic Distortion.

Introduction

Nowadays, the AC machine has replaced the DC machine in the industrial applications because of its advantages, such as, the reliability and the lack of commutator and brushes which make it able to work under unfriendly conditions [1]. The most popular AC machines are the induction motors and the permanent magnet synchronous motors. They are used in various industrial applications, electric vehicles, tools and drives. The squirrel cage induction motor in particular, is widely used due to its reduced cost and lower maintenance requirement [2].

Generally, the control and estimation of the induction motor in variable speed operation is more complicated than the DC motor, because they have more complex dynamic and they request more complicated calculations. The direct torque control is the most known control algorithm in literature for variable-speed AC

motors [3]. The DTC technique was introduced in the middle of the 80s as an alternative of the vector control because of many advantages, such as the simpler structure, the faster dynamic response and the less dependence to machine parameters [4].

However, the basic DTC strategy has a variable switching frequency, consequently, it causes non-desired ripples in flux and torque [5]. The augmentation of number of sectors is among the proposed solutions to overcome this drawback, where it can reduce the ripples by providing a constant switching voltage [6]. This technique has a very quick response time and is very effective [7].

This paper is structured as follows: section 1 introduces the topic and the literature review. Section 2 details the materials and methods. First, the induction motor modeling. Then, the DTC improvement technique. Section 3 highlights the obtained results and presents a full discussion. Section 4 concludes the paper.

Materials and methods

Induction Motor Modelling

The induction motor has many state-space mathematical models, each model is expressed by assuming a certain state vector. The modeling of AC machines is mainly based on the work of G. Kron, who gave birth to the concept of generalized machine as described in reference [8]. Park's model is a special case of this concept. It is often used for the synthesis of control laws and estimators. Described by a non-linear algebra-differential system, Park's model reflects the dynamic behavior of the electrical and electromagnetic modes of the induction machine. It admits several classes of state representations. These model classes depend directly on the control objectives (torque, speed, position), the nature of the power source of the work repository and the choice of state vector components (flux or currents, stator or rotor). In this paper, the mathematical model of the machine in use is described in the stator fixed reference frame (stationary frame) by assuming the stator currents and the rotor fluxes as state variables [9].

The mathematical model of a three-phase squirrel cage induction motor drive in α-β reference frame is:

$$\begin{cases} \dot{X} = AX + BU \\ \quad Y = CX \end{cases} \tag{1}$$

Where X, U and Y are the state, the input, and the output vector respectively:

$$X = \begin{bmatrix} i_{\alpha s} & i_{\beta s} & \phi_{\alpha r} & \phi_{\beta r} \end{bmatrix}^t; \ U = \begin{bmatrix} u_{\alpha s} & u_{\beta s} \end{bmatrix}^t;$$

$$Y = \begin{bmatrix} i_{\alpha s} & i_{\beta s} \end{bmatrix}^t;$$

$$A = \begin{bmatrix} -a_1 & \omega_s & a_2 & a_3\omega_r \\ -\omega_s & -a_1 & -a_3\omega_r & a_2 \\ a_4 & 0 & a_5 & \omega_r \\ 0 & a_4 & -\omega_r & -a_5 \end{bmatrix};$$
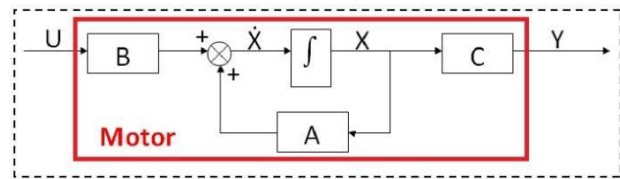
$$B = \begin{bmatrix} \dfrac{1}{\sigma L_s} & 0 \\ 0 & \dfrac{1}{\sigma L_s} \\ 0 & 0 \\ 0 & 0 \end{bmatrix}$$

$$C = \begin{bmatrix} 1 & 0 & 0 & 0 \\ 0 & 1 & 0 & 0 \end{bmatrix}$$

With $a_1 = \dfrac{R_s}{\sigma L_s} + \dfrac{R_r L_m^2}{\sigma L_s L_r}; \ a_2 = \dfrac{L_m}{\sigma L_s L_r \tau_r}; \ a_3 = \dfrac{L_m}{\sigma L_s L_r};$

$a_4 = \dfrac{L_m}{\tau_r}; \ a_5 = \dfrac{1}{\tau_r}; \ \tau_r = \dfrac{L_r}{R_r}$

The state space mathematical model of the induction motor is shown in the Figure 1.

Figure 1. Induction motor state-space mathematical model.

DTC Improvement

Conventional DTC

Based on the model of the induction motor in a stationary reference frame, the stator flux can be expressed by:

$$\frac{d\phi_s}{dt} = V_s - R_s i_s \tag{2}$$

$$\phi_s(t) = \int_0^{T_z} (V_s - R_s i_s)dt + \phi_s(0) \tag{3}$$

Where $\phi_s(0)$ is the flux vector at instant $t = 0$ and T_z is the sampling time. By applying a non-zero vector in the sampling period T_z, we can neglect the voltage drop of the stator resistance $Rsis$ with respect to V_s for the high-speed regions. Equation (3) can be then written as:

$$\phi_s(t) \approx V_s T_z + \phi_s(0) \tag{4}$$

The relationship between stator voltage and its variation in stator flux can be established as follows:

$$\Delta\phi_s = \phi_s(t) - \phi_s(0) = V_s T_z \tag{5}$$

Equation (5) means that the stator flux can be varied by applying stator voltage for a time T_z. The end of the stator flux vector moves in the direction given by the voltage vector and makes a circular path, as shown in the Figure 2.

A two-level hysteresis comparator is used for the flux control. This makes it easy to drop the end of the flux vector within the boundaries of the two near-radius concentric circles, as shown in the Figure 3 [10].
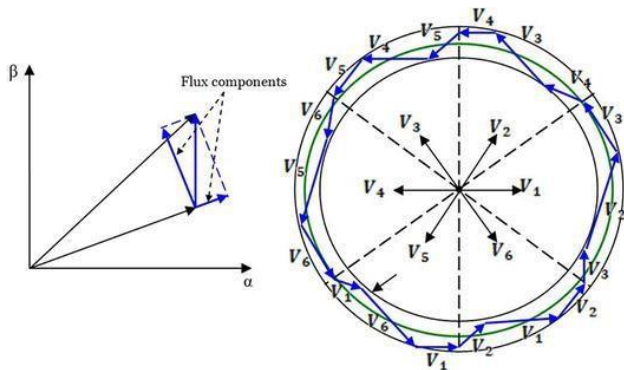
Figure 2. Evolution of the stator flux vector in the complex plan.
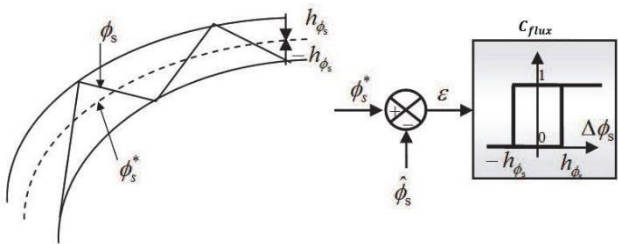
Figure 3. Two-levels comparator for the stator flux control.

The logic outputs of the flux controller are defined as:

$$\begin{cases} C_{flux} = 1 \ \ if \ \ \Delta\phi_s > +h_{\phi_s} \\ C_{flux} = 0 \ \ if \ \ \Delta\phi_s \leq -h_{\phi_s} \end{cases} \tag{6}$$

With h_{ϕ_s} is the hysteresis band of the stator flux. The choice of the hysteresis bandwidth h_{ϕ_s} depends on the switching frequency of the inverter. During a sampling period, the rotor flux vector is assumed to be invariant. The torque of the induction motor can be expressed in terms of stator and rotor flux vectors, as follows:

$$T_e = p \frac{M_{sr}}{\sigma L_s L_r} \phi_s \times \phi_r \tag{7}$$

$$T_e = p \frac{M_{sr}}{\sigma L_s L_r} |\phi_s||\phi_r|\sin(\delta) \tag{8}$$

Where, p is the number of pole pairs, ϕ_s and ϕ_r are the vectors of stator and rotor flux. δ is the angle between the vectors of the stator and rotor fluxes.

From (8), it is clear that the electromagnetic torque is controlled by the magnitudes of the stator and rotor fluxes. If these quantities remain constant, the torque can be controlled by just adjusting the angle δ. The torque control can be achieved using a three-levels hysteresis comparator as shown in the Figure 4.
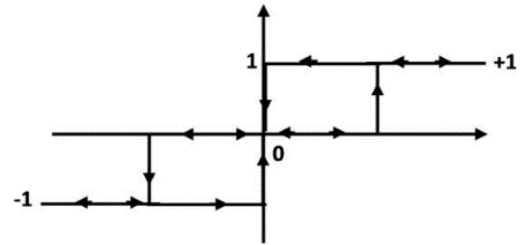
Figure 4. Three-levels hysteresis comparator for torque control.

It allows the motor to be controlled in both directions of rotation. While the two-level comparator can only be used for one direction of rotation. The logic outputs of the torque controller are defined as follows:

$$\begin{cases} C_{T_e} = 1 \ \ if \ \ \Delta T_e > +h_{T_e} \\ C_{T_e} = 0 \ \ if \ \ \Delta T_e \leq -h_{T_e} \end{cases} \tag{9}$$

C_{T_e} is the hysteresis band of torque. To maintain decoupled control, two hysteresis comparators receive stator flux and input torque errors. Then, the outputs of the comparators determine the selection of the appropriate voltage vector. However, the choice of voltage vector depends not only on the output of the hysteresis controllers, but also on the position of the stator flux vector. Thus, the vector path of the circular stator flux will be divided into six symmetrical sectors. While the stator flux vector is located in the sector i we have:

- If V_{i+1} is selected, ϕ_s increases and T_e increases.
- If V_{i-1} is selected, ϕ_s increases and T_e decreases.
- If V_{i+2} is selected, ϕ_s decreases and T_e increases.
- If V_{i-2} is selected, ϕ_s decreases and T_e decreases.

Figure 5 shows that for each sector the vectors V_i and V_{i+3} are not taken into account, as they can both increase or decrease the torque in the same sector depending on the position of the flux vector on the first or the second sector. If the null vectors V_0 and V_7 are selected, the stator flux will stop moving and its amplitude will not change, the torque will decrease, but not as much as when the active voltage vector are selected.

Twelve Sectors DTC for Ripples Reduction

In the conventional DTC, two switching states per sector are not taken into account (V_i and V_{i+3}), and this presents an ambiguity in the torque control. To solve the problem of ambiguity in torque and flux, the position of the stator flux should be divided into 12 sectors instead of 6 as shown in the Figure 6 [11].
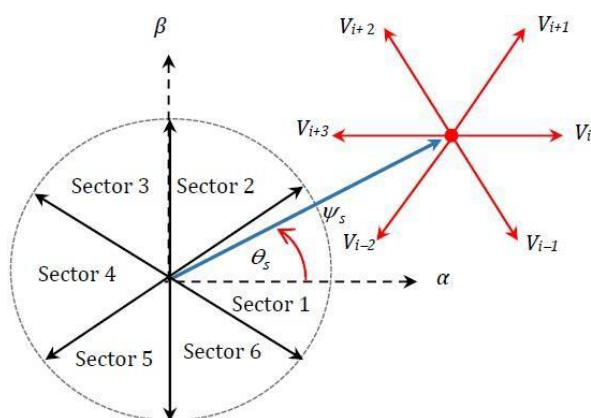
Figure 5. Voltage vector selection when the flux vector is located in the sector i.
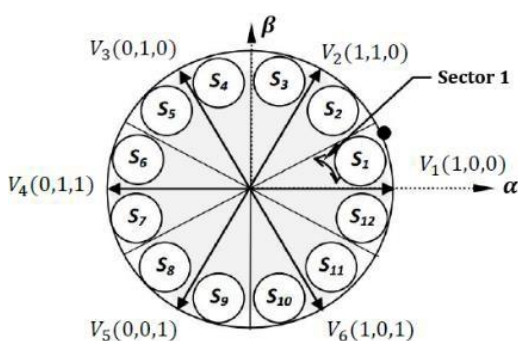
**Figure 6.** Voltage space vector in twelve sectors partition.

The main advantage of this new distribution is that all the six active vectors will be used in the same sector. However, the tangential component of the voltage vector is very low, therefore the torque variation will also be low. For this, we must introduce the idea of small torque increase instead of torque increase [12]. The new partition is detailed in the Figure 7.
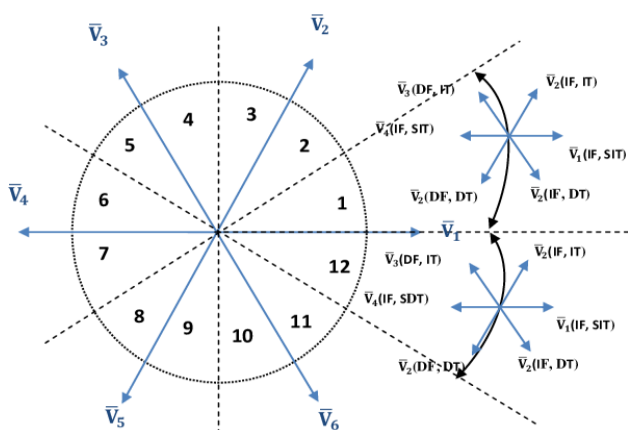
Figure 7. Voltage space vector in the new partition.

To better exploit these voltages, a four-level hysteresis comparator is used for the torque control as

illustrated in the Figure 8, which makes it possible to define the small and large variations in torque and flux generated by these same voltage vectors according to their phase shift with respect to zone boundaries [13]. For example, in sector S_{12}, if the vector V_1 is selected it will produce a large increase in flux and a small increase in ,torque, and V_2 greatly increases torque and slightly increases flux. In twee sectors DTC, the vector V_1 produces a large increase in flux and a slight increase in torque for the sector 12. On the contrary, V_2 produces a large increase in torque and low flux. It can be deduced from this that it is now necessary to define small and large variations in torque. This requires dividing the torque hysteresis band into four parts [14]. Next, a twelve-sectors new switching table is provided (Table 1).
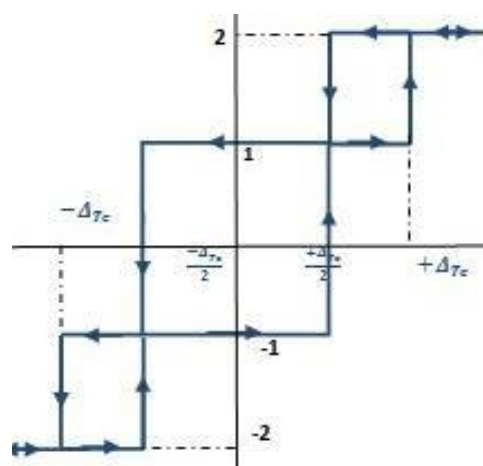
Figure 8. Four-levels torque hysteresis comparator.

Numerous studies have indicated that increasing the number of sectors has a slight effect in reducing high ripples and current harmonics [14], [15].

Table 1. The proposed twelve-sectors switching table.

| ϕ_s	T_{em}	S_1	S_2	S_3	S_4	S_5	S_6	S_7	S_8	S_9	S_{10}	S_{11}	S_{12}
	+2	V_2	V_3	V_3	V_4	V_4	V_5	V_5	V_6	V_6	V_1	V_1	V_2
1	+1	V_2	V_2	V_3	V_3	V_4	V_4	V_5	V_5	V_6	V_6	V_1	V_1
	-1	V_1	V_1	V_2	V_2	V_3	V_3	V_4	V_4	V_5	V_5	V_6	V_6
	-2	V_6	V_1	V_1	V_2	V_2	V_3	V_3	V_4	V_4	V_5	V_5	V_6
	+2	V_3	V_4	V_4	V_5	V_5	V_6	V_6	V_1	V_1	V_2	V_2	V_3
0	+1	V_4	V_4	V_5	V_5	V_6	V_6	V_1	V_1	V_2	V_2	V_3	V_3
	-1	V_5	V_5	V_6	V_6	V_1	V_1	V_2	V_2	V_3	V_3	V_4	V_4
	-2	V_5	V_6	V_6	V_1	V_1	V_2	V_2	V_3	V_3	V_4	V_4	V_5

Results and Discussion

The proposed DTC have been simulated by MATLAB/Simulink. A comparative study between the conventional and the improved technique is presented. The simulation has been conducted for three phases $3\ kW$ squirrel-cage induction motor with characteristics given in the appendix. A special analysis using the Fast Fourier Transform (FFT) is established to detect the torque and the flux harmonic order. The test in Figure 8 shows the starting up of the induction motor according to a very low speed reference of $10\ rad/s$. Then, a load of $10\ Nm$ is applied at $t=0.6s$ and removed at $t=1.6s$.

The simulation results show that both techniques have good dynamic at starting up. We can notice that the speed regulation loop rejects the applied load quickly. The convent   ional DTC kept the same fast speed response as the modified strategy. There is no difference in the transient response since the same PI speed controller is used for both schemes. The conventional DTC in the Figure 10 shows a chopped sinusoid waveform of the torque and the flux which indicates the high harmonics level, while the modified version shows a smoother sinusoid waveform. It can be justified in the Figure 9 where the modified DTC has a lower THD level, 91.36% in Figure 9 (b) compared to 123.62% for the conventional version in Figure 9 (a). The stator flux shows an acceptable waveform but high ripples level, the modified DTC shows a reducer flux ripples than the classical, **33.50%** in Figure 9 (d) compared to **64.53%** for the conventional DTC in Figure 9 (c).

Conclusion

A modified DTC for induction motor ripples reduction is designed and simulated, and its dynamic performance is studied too. The torque pulsation and the flux distortion are much better with the proposed technique. The simulated responses show that the system performance is good during the sudden load application. The flux and the torque during the steady state are improved, with faster dynamic characteristic. The modified DTC showed a reducer flux ripples, faster magnitude tracking at the starting up and better components waveform than the conventional DTC. In conclusion, this technique has proved good performance. dynamic operation
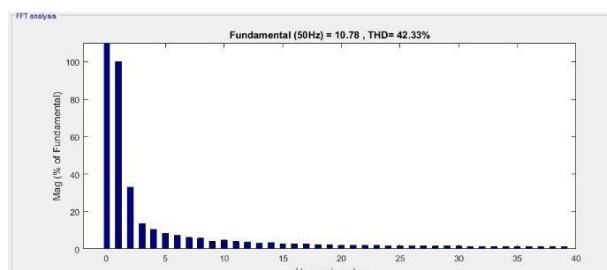
(a) Conventional DTC: Torque THD.
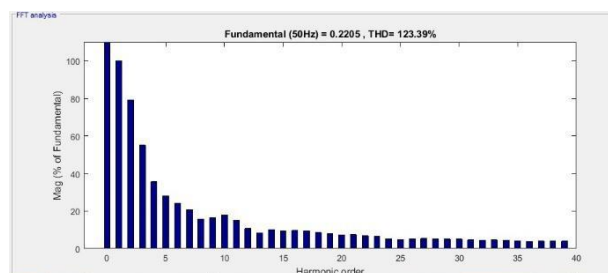
(b) Modified DTC: Torque THD.
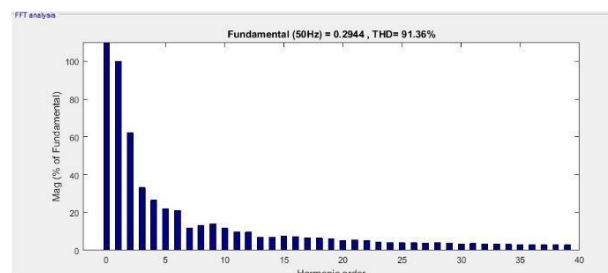
(c) Conventional DTC: Flux THD.
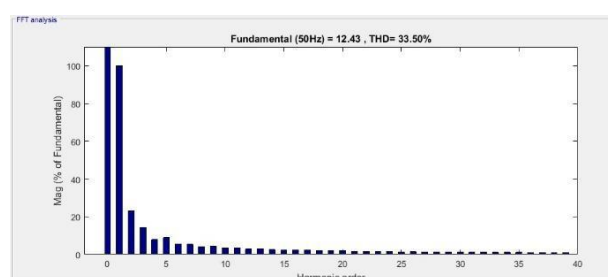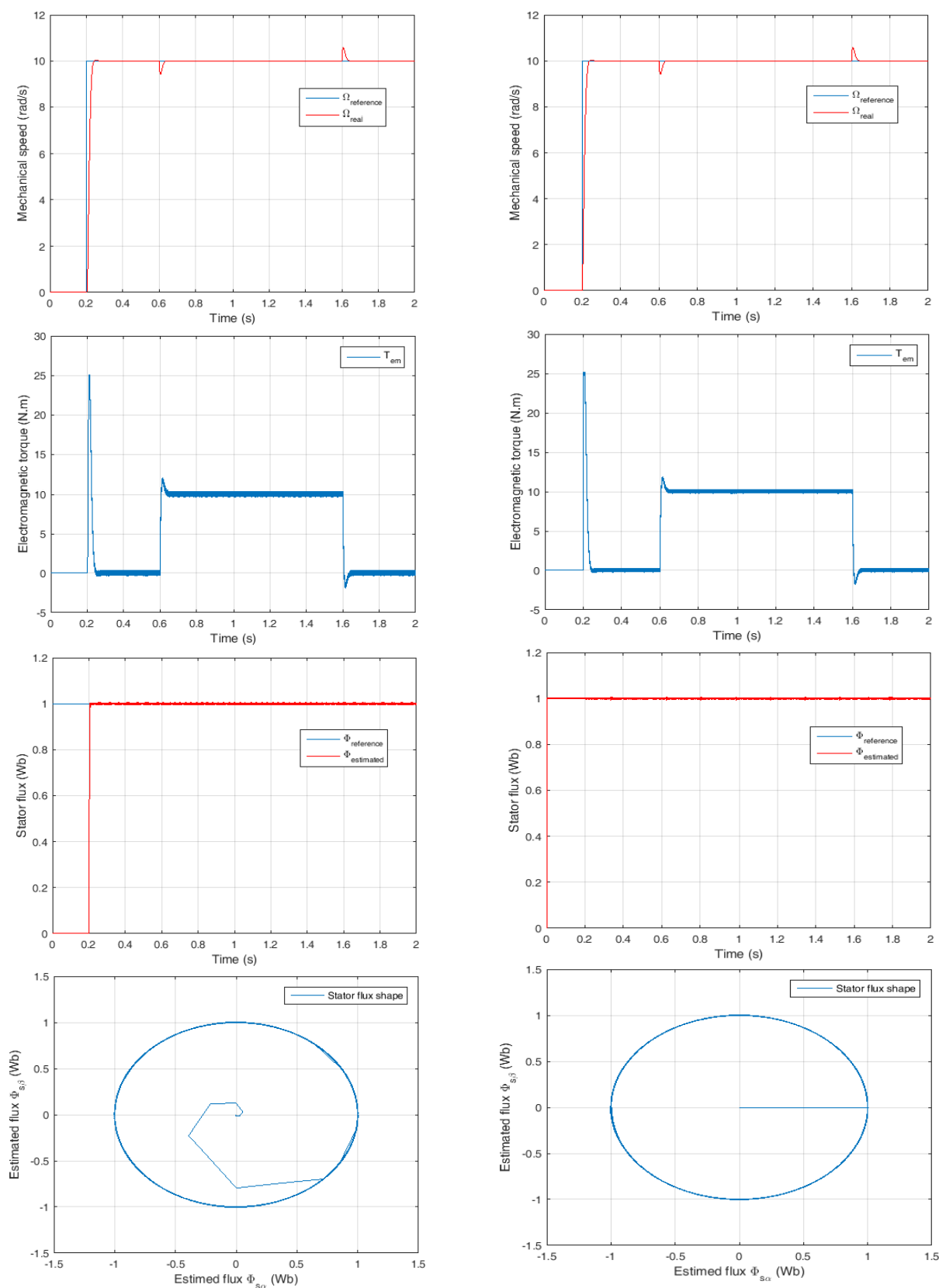

(d) Modified DTC: Flux THD.

Figure 9. Torque and flux THD improvement.

Figure 10. Conventional versus modified DTC: Test at low-speed region

Appendix

Rated power	$3\ kW$
Frequency	$50\ H_Z$
Pole pair	2
Rated speed	$1440\ rpm$
Stator resistance	$2.2\ \Omega$
Rotor resistance	$2.68\ \Omega$
Stator inductance	$0.229\ H$
Rotor inductance	$0.229\ H$
Mutual inductance	$0.217\ H$
Inertia moment	$0.074\ kg.m^2$
Viscous friction coefficient	$0.004\ N.rad/s$

References

[1]   N. P. Quang, and D. Jörg-Andreas, Vector control of three-phase AC machines, vol. 2, Heidelberg: springer, 2008.

[2]   R. Marino, T. Patrizio, and M. V. Cristiano, Induction motor control design, Springer Science and Business Media, 2010. https://doi.org/10.1007/978-1-84996-284-1

[3]   A. M. Trzynadlowski, Control of induction motors, Elsevier, 2000. https://doi.org/10.1016/B978-012701510-1/50003-9

[4]   P. Vas, Sensorless vector and direct torque control, Oxford Univ. Press, 1998.

[5]   G. S. Buja and P. K. Marian, "Direct torque control of PWM inverter-fed AC motors-a survey", *IEEE Transactions on industrial electronics*, vol. 51, no. 4, pp. 744–757, 2004. https://doi.org/10.1109/TIE.2004.831717

[6]   Y. User, K. Gulmez, and S. Ozen, "Sensorless twelve sector implementation of DTC controlled IM for torque ripple reduction", in proceeding of *6th international Advanced Technologies Symposium*, 2011.

[7]   F. Wang, Z. Zhang, X. Mei, J. Rodríguez, and R. Kennel, "Advanced control strategies of induction machine: Field oriented control, direct torque control and model predictive control", *Energies*, vol. 11, no. 1, 120, 2018. https://doi.org/10.3390/en11010120

[8]   G. Kron, "Generalized theory of electrical machinery", *Transactions of the American Institute of Electrical Engineers*, vol. 49, no. 2, pp. 666–683, 1930. https://doi.org/10.1109/T-AIEE.1930.5055554

[9]   Y. Zahraoui, M. Akherraz, C. Fahassa, and S. Elbadaoui, "Robust control of sensorless sliding mode-controlled induction motor drive facing a large-scale rotor resistance variation". In Proceedings of the *4th International Conference on Smart City Applications*, pp. 1-6, 2019. https://doi.org/10.1145/3368756.3369036

[10]   Y. Zahraoui, M. Akherraz, C. Fahassa, "Induction motor performance improvement using twelve sectors DTC and fuzzy logic speed regulation", *WSEAS Transactions on Systems and Control*, vol. 15, pp. 47– 56, 2020. https://doi.org/10.37394/23203.2020.15.6

[11]   S. Huang, G. Wu, F. Rong, C. Zhang, S. Huang, Q. Wu, "Novel predictive stator flux control techniques for PMSM drives", *IEEE Transactions on Power Electronics*, vol. 34, no. 9, pp. 8916–8929, 2018. https://doi.org/10.1109/TPEL.2018.2884984

[12]   Y. Zahraoui, M. Akherraz, C. Fahassa, "Induction Motor DTC Performance Improvement by Reducing Torque Ripples in Low Speed", *UPB Sci. Bull., Series C*, vol. 81, no. 3, pp. 249–260, 2019.

[13]   Y. Cho, B. Yeongsu, L. Kyo-Beum, "Torque-ripple reduction and fast torque response strategy for predictive torque control of induction motors", *IEEE Transactions on Power Electronics*, vol. 33, pp. 2458–2470, 2017. https://doi.org/10.1109/TPEL.2017.2699187

[14]   Y. Xiaoqing, X. Du, L. Sun, "Improved duty-ratio stator- flux eighteen-sector SVM-DTC system for new type TFPM", *International Conference on Advanced Mechatronic Systems*, IEEE. https://doi.org/10.1109/ICAMechS.2018.8507139

[15]   Z. Wu, J. Zhou, G. Zheng, T. Li, Z. Zhu, "New Eighteen- sector Direct Torque Control Based on Duty Ratio Modulation", *Journal of Physics: Conference Series*, vol. 1449, no. 1, 2020. https://doi.org/10.1088/1742-6596/1449/1/012033